Smart Structures and Systems, *Vol. 31*, *No. 2* (*2023*) *131-140*
https://doi.org/10.12989/sss.2023.31.2.131

An improved extended Kalman filter for parameters and loads identification without collocated measurements

Jia He*, Mengchen Qi, Zhuohui Tong, Xugang Hua and Zhengqing Chen

Key Laboratory of Building Safety and Energy Efficiency of the Ministry of Education,
Key Laboratory of Wind and Bridge Engineering of Hunan Province, *Hunan University*, *Changsha*, *China*

(*Received November 25*, *2021*, *Revised August 26*, *2022*, *Accepted October 15*, *2022*)

Abstract. As well-known, the extended Kalman filter (EKF) is a powerful tool for parameter identification with limited measurements. However, traditional EKF is not applicable when the external excitation is unknown. By using least-squares estimation (LSE) for force identification, an EKF with unknown input (EKF-UI) approach was recently proposed by the authors. In this approach, to ensure the influence matrix be of full column rank, the sensors have to be deployed at all the degrees-of-freedom (DOFs) corresponding to the unknown excitation, saying collocated measurements are required. However, it is not easy to guarantee that the sensors can be installed at all these locations. To circumvent this limitation, based on the idea of first-order-holder discretization (FOHD), an improved EKF with unknown input (IEKF-UI) approach is proposed in this study for the simultaneous identification of structural parameters and unknown excitation. By using projection matrix, an improved observation equation is obtained. Few displacement measurements are fused into the observation equation to avoid the so-called low-frequency drift. To avoid the ill-conditioning problem for force identification without collocated measurements, the idea of FOHD is employed. The recursive solution of the structural states and unknown loads is then analytically derived. The effectiveness of the proposed approach is validated via several numerical examples. Results show that the proposed approach is capable of satisfactorily identifying the parameters of linear and nonlinear structures and the unknown excitation applied to them.

Keywords: data fusion; first-order-holder discretization; improved EKF; parameters identification; unknown input

1. Introduction

Parameter identification plays an important role in the field of structural health monitoring (SHM). The identified parameters can be used for damage detection, condition assessment and remaining service-life prediction. To date, there are a number of methods performed in frequency domain, time domain or time-frequency domain for parameter identification (Xu and He 2017, Das and Saha 2018, Hannan *et al*. 2018). The Kalman filter (KF) provides an effective way for the estimation of structural states (Xu *et al*. 2016, Lai *et al*. 2016, Zhang *et al*. 2021, Saleem and Jo 2021). However, the structural parameters in KF algorithms should be assumed to be known. The extended Kalman filter (EKF) methods treat the parameters to be identified as a part of structural states and directly identify them in a recursive manner. The structural damage including its existence, location and severity can be then estimated on the basis of these identified quantities.

The research on the development of EKF technique for the purpose of SHM has been conducted for many years. In the classic EKF methods, the external excitation should be assumed to be known. The earlier contribution to the identification of structural parameters using EKF can be traced back to the work by Yun and Shinozuka (1980). A weighted global iteration EKF (WGI-EKF) procedure was then presented by Hoshiya and Saito (1984) to ensure the convergence and stability of the EKF algorithm. In the last century, computational efficiency may be the greatest obstacle for the application of EKF technique due to the complexity of calculating Jacobian matrix. In the past two decades, as the rapid advances of computer technologies, EKF algorithm has been actively investigated and widely used for parameter identification. For example, an improved EKF approach was proposed by Lei *et al*. (2014) for impact-induced damage detection. Mu and Yuen (2015) proposed an outlier-resistant EKF approach for the online identification of structural parameters. With the combination of EKF and UKF, Liu *et al*. (2016) proposed a two-stage approach to identify the nonlinear structural parameters. A discontinuous EKF method was presented by Chatzis *et al*. (2017) for state estimation and parameters identification. Based on EKF and *l*1-norm regularization, Zhang *et al*. (2017) proposed an algorithm for detecting local damage of complex structures. More recently, Lei *et al*. (2018) proposed an EKF-based approach for damage detection under ambient excitation. Ginsberg *et al*. (2018) proposed a sparsity-constrained EKF approach for damage localization and identification. An adaptive EKF with two computational modes was proposed by Yang *et al*. (2020) for system identification under seismic inputs. Based on WGI-EKF procedure, Xu *et al*. (2020) proposed a

*Corresponding author, Associate Professor,
E-mail: jiahe@hnu.edu.cn

ISSN: 1738-1584 (Print), 1738-1991 (Online)

nonparametric approach for the identification of nonlinear hysteretic behavior. Li and Wang (2020) proposed a constraint EKF approach for parameter identification of a differentiable Bouc-Wen model. Based on unscented KF, Naranjo-Perez *et al*. (2020) proposed a multi-objective harmony search algorithm for parameter identification of the dynamic Winkler soil-structure interaction model. Xiao *et al*. (2021) proposed an adaptive EKF approach for identifying the frequencies and track irregularities of high-speed railway bridges.

In the EKF-based approaches mentioned above, the external loads are required for the estimation. Without the prior knowledge of input information, these methods are unable to track the evolution of the estimates. However, some loads may not be measured in practice due to inaccessibility of sensor locations or other practical limitations. Therefore, much effort has been made on the development of EKF under unknown input (EKF-UI) methods. For example, Yang *et al*. (2007) proposed an adaptive EKF-UI approach for the identification of time-varying parameters. By using least-squares estimation (LSE) and EKF in sequence, Lei *et al*. (2012) proposed an EKF-UI approach for damage detection. Based on WGI-EKF and an adaptive iteration procedure, Xu and He (2015) proposed an approach for the identification of substructural parameters and unknown loads. Pan *et al*. (2016) proposed a general EKF-UI approach to reduce the restrictions of the sensor location. Liu *et al*. (2018) proposed a modal EKF-UI approach for identifying large-scale structures in real time. With the combination of augmented Kalman filter and genetic algorithm, Saleem and Jo (2019, 2021) proposed an approach for impact force identification and sensor placement. Based on LSE and EKF, He *et al*. (2020) proposed a two-stage approach for parameters identification with unknown inputs. Lei *et al*. (2021) proposed an EKF-UI approach for the identification of nonlinear restoring force in a model-free manner.

The authors have also been conducted the research on EKF-UI methods in the recent year. By using projection matrix to derive a modified observation equation, an EKF-UI approach was proposed for the simultaneous identification of structural parameters and unknown loadings (He *et al*. 2019a). It was then extended for substructural identification (He *et al*. 2021). This approach is novel and not presented in the previous literature. However, in order to ensure the influence matrix be of full column rank and to obtain the modified observation equation, sensors should be placed at all of the DOFs where the unknown inputs are applied, i.e., collocated acceleration measurements at the locations of unknown inputs are required. This limitation is also mentioned in some other literatures (Lei *et al*. 2012, Xu and He 2015, Pan *et al*. 2016, Liu *et al*. 2018). As known, it is not always possible to deploy the sensors at all these desired locations. Therefore, to circumvent this limitation, based on the idea of first-order-holder discretization (FOHD), an improved EKF with unknown input (IEKF-UI) approach is proposed in this study. Data fusion technique is employed to avoid the so-called low-frequency drift, and an improved version of observation equation is obtained. The recursive solution of the proposed approach is analytically derived. Several numerical examples including linear and nonlinear structures are used for the validation of its effectiveness.

2. Formulas of the proposed IEKF-UI approach

In general, the equation of motion of an n-DOFs structure with unknown loads can be written as

$$\boldsymbol{M}\ddot{\boldsymbol{x}}(t) + \boldsymbol{F}[\boldsymbol{x}(t), \dot{\boldsymbol{x}}(t), \boldsymbol{\theta}] = \boldsymbol{\varphi}\boldsymbol{f}(t) + \boldsymbol{\varphi}_u\boldsymbol{f}_u(t) \tag{1}$$

in which $\mathbf{M}$ is mass matrix; $\mathbf{x}(t)$, $\dot{\boldsymbol{x}}(t)$ and $\ddot{\boldsymbol{x}}(t)$ are time series of displacement, velocity and acceleration, respectively; $\boldsymbol{F}[\boldsymbol{x}(t), \dot{\boldsymbol{x}}(t), \boldsymbol{\theta}]$ is restoring force vector; $\boldsymbol{\theta}$ represents the unknown parameters; $\mathbf{f}(t)$ and $\mathbf{f}_u(t)$ are the known and unknown inputs, respectively; $\boldsymbol{\varphi}$ and $\boldsymbol{\varphi}_u$ are the influence matrices associated with the known and unknown inputs, respectively.

In this study, the parameters to be identified are assumed to be time-invariant. Thus, with the definition of the extended state vector $\boldsymbol{Z}(t) = [\boldsymbol{x}(t)^T,\ \dot{\boldsymbol{x}}(t)^T,\ \boldsymbol{\theta}^T]^T$, the following state equation can be obtained

$$\begin{aligned}\dot{\boldsymbol{Z}}(t) &= \begin{bmatrix} \dot{\boldsymbol{x}}(t) \\ \boldsymbol{M}^{-1}[-\boldsymbol{F}[\boldsymbol{x}(t), \dot{\boldsymbol{x}}(t), \boldsymbol{\theta}] + \boldsymbol{\varphi}\boldsymbol{f}(t) + \boldsymbol{\varphi}_u\boldsymbol{f}_u(t)] \\ \mathbf{0} \end{bmatrix}^T \\ &= \boldsymbol{g}(\boldsymbol{Z}(t), \boldsymbol{f}(t), \boldsymbol{f}_u(t), t) + \boldsymbol{w}(t)\end{aligned} \tag{2}$$

where $\mathbf{w}(t)$ is the process noise vector with zero mean and a covariance matrix $\mathbf{Q}(t)$.

The state equation mentioned above can be linearized as

$$\begin{aligned}&\boldsymbol{g}(\boldsymbol{Z}_k, \boldsymbol{f}_k, \boldsymbol{f}_{u,k}, k\Delta t) \\ &\approx \boldsymbol{g}(\hat{\boldsymbol{Z}}_{k|k}, \boldsymbol{f}_k, \hat{\boldsymbol{f}}_{u,k}, k\Delta t) + \boldsymbol{U}_{k|k}(\boldsymbol{Z}_k - \hat{\boldsymbol{Z}}_{k|k}) \\ &\quad + \boldsymbol{W}_{k|k}(\boldsymbol{f}_{u,k} - \hat{\boldsymbol{f}}_{u,k})\end{aligned} \tag{3}$$

where $\hat{\boldsymbol{Z}}_{k|k}$ and $\hat{\boldsymbol{f}}_{u,k}$ are the estimates of $\mathbf{Z}_k$ and $\mathbf{f}_{u,k}$ at the k-th time step, respectively; Δt is the time interval; $\mathbf{U}_{k|k}$ and $\mathbf{W}_{k|k}$ can be calculated as follows

$$\begin{aligned}\boldsymbol{U}_{k|k} &= \frac{\partial \boldsymbol{g}(\boldsymbol{Z}_k, \boldsymbol{f}_k, \boldsymbol{f}_{u,k}, k\Delta t)}{\partial \boldsymbol{Z}_k}\bigg|_{\substack{\boldsymbol{Z}_k = \hat{\boldsymbol{Z}}_{k|k} \\ \boldsymbol{f}_{u,\,k} = \hat{\boldsymbol{f}}_{u,\,k}}}, \\ \boldsymbol{W}_{k|k} &= \frac{\partial \boldsymbol{g}(\boldsymbol{Z}_k, \boldsymbol{f}_k, \boldsymbol{f}_{u,k}, k\Delta t)}{\partial \boldsymbol{f}_{u,\,k}}\bigg|_{\substack{\boldsymbol{Z}_k = \hat{\boldsymbol{Z}}_{k|k} \\ \boldsymbol{f}_{u,\,k} = \hat{\boldsymbol{f}}_{u,\,k}}} = \begin{bmatrix} \mathbf{0} \\ \boldsymbol{M}^{-1}\boldsymbol{\varphi}_u \\ \mathbf{0} \end{bmatrix}\end{aligned} \tag{4}$$

Here, partial displacement and acceleration responses are fused together and used for the identification. The discretized observation equation can be then expressed as

$$\begin{aligned}\bar{\boldsymbol{y}}_k &= \begin{bmatrix} \boldsymbol{y}_{a,k} \\ \boldsymbol{y}_{s,k} \end{bmatrix} = \begin{bmatrix} \boldsymbol{L}_a\ddot{\boldsymbol{x}}_k + \boldsymbol{v}_{a,k} \\ \boldsymbol{L}_s\boldsymbol{x}_k + \boldsymbol{v}_{s,k} \end{bmatrix} \\ &= \begin{bmatrix} \boldsymbol{L}_a(\boldsymbol{h}(\boldsymbol{Z}_k) + \boldsymbol{M}^{-1}\boldsymbol{\varphi}_u\boldsymbol{f}_{u,k}) + \boldsymbol{v}_{a,k} \\ \boldsymbol{L}_s\boldsymbol{x}_k + \boldsymbol{v}_{s,k} \end{bmatrix}\end{aligned} \tag{5}$$

where $\boldsymbol{h}(\boldsymbol{Z}_k) = \boldsymbol{M}^{-1}[-\boldsymbol{F}[\boldsymbol{x}_k, \dot{\boldsymbol{x}}_k, \boldsymbol{\theta}] + \boldsymbol{\varphi}\boldsymbol{f}_k]$; $\mathbf{L}_a$ and $\mathbf{L}_s$ are the matrices associated with the locations of accelerometers and displacement transducers, respectively; $\mathbf{y}_{a,k}$ and $\mathbf{y}_{s,k}$ are the acceleration and displacement measurements at the k-th

time step, respectively; $\mathbf{v}_{a,k}$ and $\mathbf{v}_{s,k}$ are measurement noise assumed to be Gaussian white-noise vector with zero mean and covariance matrices $\mathbf{R}_{a,k}$ and $\mathbf{R}_{s,k}$, respectively.

Focusing on the first part of the observation equation where the unknown inputs are explicitly included, the following equation regarding acceleration measurements can be obtained

$$\boldsymbol{y}_{a,k} = \boldsymbol{L}_a\big(\boldsymbol{h}(\boldsymbol{Z}_k) + \boldsymbol{M}^{-1}\boldsymbol{\varphi}_u\boldsymbol{f}_{u,k}\big) + \boldsymbol{v}_{a,k} \tag{6}$$

In this study, to investigate a general case, the unknown inputs $\mathbf{f}_{u,k}$ are considered to be composed of two parts, namely $\boldsymbol{f}^*_{u,k}$ and $\boldsymbol{f}'_{u,k}$. The former represents the unknown input vector associated with the collocated acceleration responses being measured, whereas the latter represents the unknown input vector without the collocated acceleration measurements. Then, Eq. (6) can be expressed as

$$\boldsymbol{y}_{a,k} = \boldsymbol{L}_a\boldsymbol{h}(\boldsymbol{Z}_k) - [\boldsymbol{D}^* \quad \boldsymbol{D}']\begin{bmatrix}\boldsymbol{f}^*_{u,k}\\ \boldsymbol{f}'_{u,k}\end{bmatrix} + v_{a,k} \tag{7}$$

where $\boldsymbol{D}^* = -\boldsymbol{L}_a\boldsymbol{M}^{-1}\boldsymbol{\varphi}^*_u$; $\boldsymbol{D}' = -\boldsymbol{L}_a\boldsymbol{M}^{-1}\boldsymbol{\varphi}'_u$; $\boldsymbol{\varphi}^*_u$ and $\boldsymbol{\varphi}'_u$ are the influence matrices associated with unknown input vector $\boldsymbol{f}^*_{u,k}$ and $\boldsymbol{f}'_{u,k}$, respectively. Since the matrix $\mathbf{L}_a$ is not related to the influence matrix $\boldsymbol{\varphi}'_u$, it can be found that $\boldsymbol{D}'$ matrix is always equal to zero. Then, Eq. (7) can be rearranged as follows

$$\boldsymbol{y}_{a,k} = \boldsymbol{L}_a\boldsymbol{h}(\boldsymbol{Z}_k) - \boldsymbol{D}^*\boldsymbol{f}^*_{u,k} + \boldsymbol{v}_{a,k} \tag{8}$$

Obviously, only the unknown input vector $\boldsymbol{f}^*_{u,k}$ is explicitly presented in the observation equation. For ease of expression, $\boldsymbol{f}^*_{u,k}$ is named as explicit unknown input at the k-th time step whereas $\boldsymbol{f}'_{u,k}$ is called as implicit unknown input hereafter.

Notably, the matrix $\mathbf{D}^*$ is always of full column rank. Moreover, the measurement noise is assumed to be much smaller than the measured signal. Thus, the explicit unknown input $\boldsymbol{f}^*_{u,k}$ can be estimated by LSE as follows

$$\hat{\boldsymbol{f}}^*_{u,k} = \big(\boldsymbol{D}^{*T}\boldsymbol{D}^*\big)^{-1}\boldsymbol{D}^{*T}\big[\boldsymbol{L}_a\boldsymbol{h}(\boldsymbol{Z}_k) - \boldsymbol{y}_{a,k}\big] \tag{9}$$

Then, according to the similar procedure conducted in the previous literature (He *et al*. 2019), Eq. (8) can be re-written as

$$\boldsymbol{\Phi}\boldsymbol{y}_{a,k} = \boldsymbol{\Phi}\boldsymbol{L}_a\boldsymbol{h}(\boldsymbol{Z}_k) + \boldsymbol{\Phi}\boldsymbol{v}_{a,k} \tag{10}$$

where $\boldsymbol{\Phi} = \boldsymbol{I} - \boldsymbol{D}^*\big(\boldsymbol{D}^{*T}\boldsymbol{D}^*\big)^{-1}\boldsymbol{D}^{*T}$. Here, $\boldsymbol{D}^*\big(\boldsymbol{D}^{*T}\boldsymbol{D}^*\big)^{-1}\boldsymbol{D}^{*T}$ is known as projection matrix.

On the basis of Eq. (5) and Eq. (10), an improved observation equation can be derived as

$$\bar{\boldsymbol{\Phi}}\bar{\boldsymbol{y}}_k = \bar{\boldsymbol{\Phi}}\bar{\boldsymbol{h}}(\boldsymbol{Z}_k) + \bar{\boldsymbol{\Phi}}\bar{\boldsymbol{v}}_k \tag{11}$$

where $\bar{\boldsymbol{\Phi}} = \begin{bmatrix}\boldsymbol{\Phi} & \boldsymbol{0}\\ \boldsymbol{0} & \boldsymbol{I}\end{bmatrix}$; $\bar{\boldsymbol{h}}(\boldsymbol{Z}_k) = \begin{bmatrix}\boldsymbol{L}_a\boldsymbol{h}(\boldsymbol{Z}_k)\\ \boldsymbol{L}_s\boldsymbol{x}_k\end{bmatrix}$; $\bar{\boldsymbol{v}}_k = \begin{bmatrix}\boldsymbol{v}_{a,k}\\ \boldsymbol{v}_{s,k}\end{bmatrix}$.

According to the principle of EKF, the priori state estimate $\widehat{\boldsymbol{Z}}_{k+1|k}$ can be obtained as

$$\widehat{\boldsymbol{Z}}_{k+1|k} = \widehat{\boldsymbol{Z}}_{k|k} + \int_{k\Delta t}^{(k+1)\Delta t}\boldsymbol{g}(\widehat{\boldsymbol{Z}}_{k|k}, \boldsymbol{f}_k, \hat{\boldsymbol{f}}_{u,k}, k\Delta t)dt \tag{12}$$

The priori estimate error covariance matrix $\mathbf{P}_{k+1|k}$ can be calculated as

$$\boldsymbol{P}_{k+1|k} = \boldsymbol{A}_1\boldsymbol{P}_{k|k}\boldsymbol{A}_1 + \boldsymbol{A}_2\boldsymbol{R}_{a,k}\boldsymbol{A}_2 + \Delta t^2\boldsymbol{Q}_k \tag{13}$$

where $\boldsymbol{A}_1 = \boldsymbol{I} + \Delta t\left(\boldsymbol{U}_{k|k} + \begin{bmatrix}0\\ -\boldsymbol{H}_{k|k}\\ 0\end{bmatrix}\right)$;

$\boldsymbol{A}_2 = \Delta t\begin{bmatrix}0\\ -(\boldsymbol{L}_a^T\boldsymbol{L}_a)^{-1}\boldsymbol{L}_a^T\\ 0\end{bmatrix}$; $\boldsymbol{H}_{k|k} = \frac{\partial \boldsymbol{h}(\boldsymbol{Z}_k)}{\partial \boldsymbol{Z}_k}\big|\boldsymbol{Z}_k = \widehat{\boldsymbol{Z}}_{k|k}$.

Then, the posteriori state estimate $\widehat{\boldsymbol{Z}}_{k+1|k+1}$ is determined as

$$\widehat{\boldsymbol{Z}}_{k+1|k+1} = \widehat{\boldsymbol{Z}}_{k+1|k} + \boldsymbol{G}_{k+1}\big[\bar{\boldsymbol{\Phi}}\bar{\boldsymbol{y}}_{k+1} - \bar{\boldsymbol{\Phi}}\bar{\boldsymbol{h}}\big(\widehat{\boldsymbol{Z}}_{k+1|k}\big)\big] \tag{14}$$

where $\mathbf{G}_{k+1}$ represents gain matrix and can be computed as

$$\begin{aligned}\boldsymbol{G}_{k+1} = \boldsymbol{P}_{k+1|k}\bar{\boldsymbol{H}}^T_{k+1}\bar{\boldsymbol{\Phi}}^T\big[\bar{\boldsymbol{\Phi}}\big(&\bar{\boldsymbol{H}}_{k+1|k}\boldsymbol{P}_{k+1|k}\bar{\boldsymbol{H}}^T_{k+1}\\ &+ \bar{\boldsymbol{R}}_{k+1}\big)\bar{\boldsymbol{\Phi}}^T\big]^{-1}\end{aligned} \tag{15}$$

in which $\bar{\boldsymbol{R}}_k = E(\bar{\boldsymbol{v}}_k\bar{\boldsymbol{v}}_k^T)$; $\bar{\boldsymbol{H}}_{k+1|k} = \frac{\partial \bar{\boldsymbol{h}}(\boldsymbol{Z}_{k+1})}{\partial \boldsymbol{Z}_{k+1}}\big|\boldsymbol{Z}_{k+1}\widehat{\boldsymbol{Z}}_{k+1\,|k}$

The posteriori estimate error covariance matrix $\mathbf{P}_{k+1|k+1}$ is calculated as

$$\begin{aligned}\boldsymbol{P}_{k+1|k+1} = \big(&\boldsymbol{I} - \boldsymbol{G}_{k+1}\bar{\boldsymbol{\Phi}}\bar{\boldsymbol{H}}_{k+1|k}\big)\boldsymbol{P}_{k+1|k}\big(\boldsymbol{I}\\ &- \boldsymbol{G}_{k+1}\bar{\boldsymbol{\Phi}}\bar{\boldsymbol{H}}_{k+1|k}\big)^T\\ &+ \boldsymbol{G}_{k+1}\bar{\boldsymbol{\Phi}}\bar{\boldsymbol{R}}_{k+1}(\boldsymbol{G}_{k+1}\bar{\boldsymbol{\Phi}})^T\end{aligned} \tag{16}$$

The recursive solution of the state estimation seems to be given by Eqs. (12)-(16). However, it should be noted that the unknown input in Eq. (6) is not completely determined. Only part of this input, saying the explicit unknown input $\hat{\boldsymbol{f}}^*_{u,k+1}$, can be obtained according to Eq. (9) and shown as follows.

$$\hat{\boldsymbol{f}}^*_{u,k+1} = \big(\boldsymbol{D}^{*T}\boldsymbol{D}^*\big)^{-1}\boldsymbol{D}^{*T}\big[\boldsymbol{L}_a\boldsymbol{h}(\widehat{\boldsymbol{Z}}_{k+1|k+1}) - \boldsymbol{y}_{a,k+1}\big] \tag{17}$$

The remaining part, i.e., the implicit unknown input $\boldsymbol{f}'_{u,k}$ is still unknown, which means the procedure described by Eqs. (12)-(16) can't be directly implemented. In order to identify this implicit unknown input, the idea of first-order-holder discretization (FOHD) (Ding *et al*. 2013, Lei *et al*. 2020) is employed.

In the conventional EKF-based approach, the zero-order-holder discretization (ZOHD) method is used to discretize the continuous function. The unknown force in a sampling period is assumed to be constant by using ZOHD method, and thus Eq. (12) can be expressed as

$$\begin{aligned}\widehat{\boldsymbol{Z}}_{k+1|k} = \widehat{\boldsymbol{Z}}_{k|k} &+ \int_{k\Delta t}^{(k+1)\Delta t}\boldsymbol{g}\big(\widehat{\boldsymbol{Z}}_{k|k}, \boldsymbol{f}_k, k\Delta t\big)dt\\ &+ \begin{bmatrix}\boldsymbol{0}\\ \boldsymbol{M}^{-1}\boldsymbol{\varphi}'_u\Delta t\end{bmatrix}\hat{\boldsymbol{f}}'_{u,k} + \begin{bmatrix}\boldsymbol{0}\\ \boldsymbol{M}^{-1}\boldsymbol{\varphi}^*_u\Delta t\end{bmatrix}\hat{\boldsymbol{f}}^*_{u,k}\end{aligned} \tag{18}$$

Different from ZOHD method, FOHD method treats the unknown input as a linear variable in a sampling period. For ease of distinction, the priori state estimate is called as $\bar{\boldsymbol{Z}}_{k+1|k}$ in this case, and Eq. (12) can be arranged as

$$\begin{aligned}\bar{\boldsymbol{Z}}_{k+1|k} = \hat{\boldsymbol{Z}}_{k|k} + \int_{k\Delta t}^{(k+1)\Delta t} \boldsymbol{g}\left(\hat{\boldsymbol{Z}}_{k|k}, \boldsymbol{f}_k, k\Delta t\right)dt \\ + \frac{1}{2}\Delta t\left(\begin{bmatrix}\boldsymbol{0}\\ \boldsymbol{M}^{-1}\boldsymbol{\varphi}_u'\end{bmatrix}\left(\hat{\boldsymbol{f}}_{u,k}' + \hat{\boldsymbol{f}}_{u,k+1}'\right)\right. \\ \left. + \begin{bmatrix}\boldsymbol{0}\\ \boldsymbol{M}^{-1}\boldsymbol{\varphi}_u^*\end{bmatrix}\left(\hat{\boldsymbol{f}}_{u,k}^* + \hat{\boldsymbol{f}}_{u,k+1}^*\right)\right)\end{aligned} \tag{19}$$

By using Eqs. (18)-(19), the following relationship exists

$$\begin{aligned}&\bar{\boldsymbol{Z}}_{k+1|k} - \hat{\boldsymbol{Z}}_{k+1|k} \\ &= \frac{1}{2}\Delta t\left[\boldsymbol{B}'\left(\hat{\boldsymbol{f}}_{u,k+1}' - \hat{\boldsymbol{f}}_{u,k}'\right) + \boldsymbol{B}^*\left(\hat{\boldsymbol{f}}_{u,k+1}^* - \hat{\boldsymbol{f}}_{u,k}^*\right)\right]\end{aligned} \tag{20}$$

where $\boldsymbol{B}' = \begin{bmatrix}\boldsymbol{0}\\ \boldsymbol{M}^{-1}\boldsymbol{\varphi}_u'\end{bmatrix}; \boldsymbol{B}^* = \begin{bmatrix}\boldsymbol{0}\\ \boldsymbol{M}^{-1}\boldsymbol{\varphi}_u^*\end{bmatrix}$.

Based on the Taylor series, Eq. (8) can be linearized as follows

$$\begin{aligned}&\boldsymbol{y}_{a,k+1} - \boldsymbol{L}_a\boldsymbol{h}(\boldsymbol{Z}_{k+1}) + \boldsymbol{D}^*\boldsymbol{f}_{u,k+1}^* = \boldsymbol{y}_{a,k+1} \\ &-\left[\boldsymbol{L}_a\boldsymbol{h}\left(\hat{\boldsymbol{Z}}_{k+1|k}\right) + \boldsymbol{L}_a\boldsymbol{H}_{k+1|k}\left(\bar{\boldsymbol{Z}}_{k+1|k} - \hat{\boldsymbol{Z}}_{k+1|k}\right)\right] \\ &+\boldsymbol{D}^*\boldsymbol{f}_{u,k+1}^* \approx 0\end{aligned} \tag{21}$$

Substituting Eq. (20) into Eq. (21) leads to

$$\begin{aligned}&\boldsymbol{y}_{a,k+1} - \boldsymbol{L}_a\boldsymbol{h}\left(\hat{\boldsymbol{Z}}_{k+1|k}\right) \\ &-\frac{1}{2}\boldsymbol{L}_a\boldsymbol{H}_{k+1|k}\Delta t\left[\boldsymbol{B}'\left(\hat{\boldsymbol{f}}_{u,k+1}' - \hat{\boldsymbol{f}}_{u,k}'\right) + \boldsymbol{B}^*\left(\hat{\boldsymbol{f}}_{u,k+1}^* - \hat{\boldsymbol{f}}_{u,k}^*\right)\right] \\ &+\boldsymbol{D}^*\hat{\boldsymbol{f}}_{u,k+1}^* = 0\end{aligned} \tag{22}$$

Then, with proper transformation, the implicit unknown input can be obtained as

$$\begin{aligned}\hat{\boldsymbol{f}}_{u,k+1}' = \left(\boldsymbol{S}_{k+1}^T\boldsymbol{S}_{k+1}\right)^{-1}\boldsymbol{S}_{k+1}^T\left[\boldsymbol{y}_{a,k+1} - \boldsymbol{L}_a\boldsymbol{h}\left(\hat{\boldsymbol{Z}}_{k+1|k}\right)\right. \\ -\frac{1}{2}\boldsymbol{L}_a\boldsymbol{H}_{k+1|k}\Delta t\left(\boldsymbol{B}^*\left(\hat{\boldsymbol{f}}_{u,k+1}^* - \hat{\boldsymbol{f}}_{u,k}^*\right)\right. \\ \left.\left. - \boldsymbol{B}'\hat{\boldsymbol{f}}_{u,k}'\right) + \boldsymbol{D}^*\hat{\boldsymbol{f}}_{u,k+1}^*\right]\end{aligned} \tag{23}$$

where $\boldsymbol{S}_{k+1} = \frac{1}{2}\boldsymbol{L}_a\boldsymbol{H}_{k+1|k}\boldsymbol{B}'\Delta t$. It can be found that the matrix $\mathbf{S}_{k+1}$ is always of full column rank.

In summary, the equations for the proposed IEKF-UI approach fall into three groups: time update equations, measurement update equations, and force identification equations. The time update equations including Eqs. (12)-(13) are responsible for the determination of a priori estimate using the information of previous time step. The measurement update equations including Eqs. (14)-(16) are responsible for incorporating a new measurement into the priori estimate to obtain an improved posteriori estimate. These two update equations are similar to those in the conventional EKF algorithm. Moreover, the unknown inputs can be identified by Eq. (17) and Eq. (23) at the same time. It can be seen that the collocated acceleration measurements are not necessarily required for the identification indicating the restriction on the sensor locations is removed. For ease of understanding, the flowchart of the proposed IEKF-UI approach is plotted in Fig. 1.

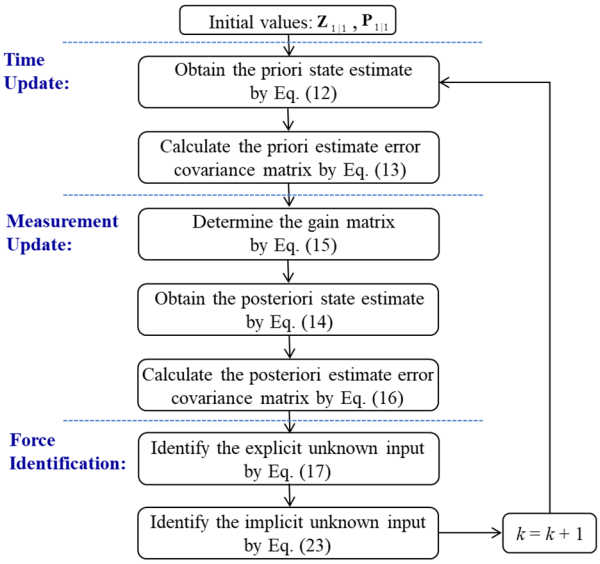

Fig. 1 The flowchart of the proposed IEKF-UI approach

3. Numerical validation

In order to validate the effectiveness of the proposed approach, several numerical examples including a shear building structure, a planar truss structure and a building structure with a nonlinear hysteretic model are considered in this section.

3.1 Eight-story shear building structure

A numerical study of an 8-story shear building structure subject to two unknown inputs is first conducted herein. The parameters of mass and stiffness are given as m_i = 180 kg and k_i = 550 kN/m (i = 1, …, 8). The Rayleigh damping model (i.e., $\mathbf{C} = \alpha\cdot\mathbf{M} + \beta\cdot\mathbf{K}$) is employed, and the proportional coefficients of α and β are assumed to be 0.457 and 1.5×10^{-3}, respectively. The first two damping ratios are 3%, and the first three natural frequencies are 1.62 Hz, 4.82 Hz and 7.84 Hz, respectively. The random external forces are applied on 2nd floor and 8th floor of the building. The corresponding structural responses are obtained by state-space method with the time interval of 0.001 s. After the calculation of structural responses, these two external forces are considered as the unknown inputs to be identified. The system error covariance matrix $\mathbf{Q}$ in this study is set to be $10^{-6}\cdot\mathbf{I}$.

The acceleration responses of the 1st, 2nd, 3rd, 6th and 7th are assumed to be known for the identification. Since the acceleration response of the 2nd floor are available, the

Table 1 The identified structural parameters of shear building

Parameters (kN/m)	Actual	Identified	Error (%)	Parameters (kN/m)	Actual	Identified	Error (%)
k_1	550	546.05	-0.72	k_6	550	554.64	0.84
k_2	550	551.71	0.31	k_7	550	544.62	-0.98
k_3	550	544.71	-0.96	k_8	550	555.56	1.01
k_4	550	546.62	-0.61	α	0.4577	0.4650	1.59
k_5	550	543.44	-1.19	β	0.0015	0.0012	-

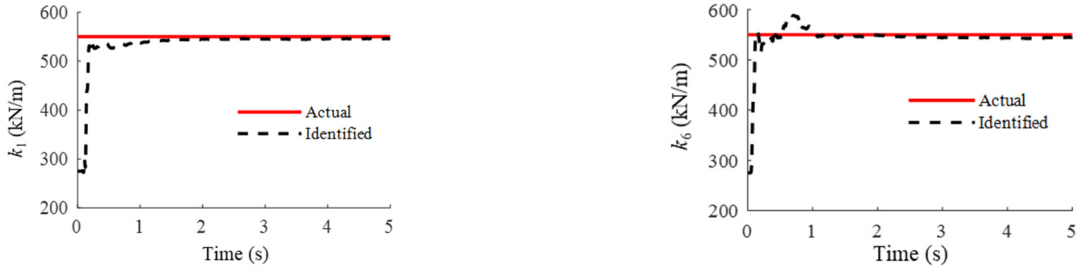

(a) The 1st floor (b) The 6th floor

Fig. 2 The identified stiffness of shear building structure

(a) On the 2nd floor (b) On the 8th floor

Fig. 3 The comparison of the identified excitation applied to shear structure

external force applied to this floor can be viewed as the explicit unknown input. Accordingly, the external force on the 8th floor can be treated as the implicit unknown input. Moreover, the displacement responses of the 1st and 6th floor are fused in the observation equation. The noise effect is considered by adding white noise with 5% in root mean square (RMS) to these measurements.

The extended state vector is defined as $\boldsymbol{Z} = [x_1,\ldots, x_8, \dot{x}_1,\ldots, \dot{x}_8, k_1,\ldots, k_8, \alpha, \beta]^T$, where x_i, $\dot{x}_i$ and k_i (i = 1, …, 8) represent the displacement, velocity and stiffness of the i-th floor, respectively. The initial values of structural parameters are assumed to be 50% of the actual ones. By using the proposed approach, the structural parameters can be identified and shown in Table 1. It can be seen that the identified values are close to the actual ones. Notably, since the value of β is several orders of magnitude smaller than other variables, it is not easy to obtain the accurate identification result of such a small coefficient. Sever strategies may be helpful for improving the accuracy of the identified result, such as reducing the noise level, using more sensors, and changing the locations of sensors. Figs. 2(a)-(b) gives the convergence details of the identified parameters. It is obvious that the identified parameters are able to stably converge to the actual ones after few seconds. Only the stiffness coefficients of the 1st and 6th floor are plotted in Figs. 2(a)-(b) as examples. Similar results can be found for the remaining parameters.

In addition to the identification of structural parameters, the unknown inputs can be also estimated by the proposed approach. The comparison of the identified external forces with their real ones is plotted in Figs. 3(a)-(b). Obviously, the identified results have a good agreement with the actual ones. Moreover, a normalized root-mean-square-error (NRMSE) (He *et al.* 2019b) is used as a measure of deviation between the actual inputs and the identified ones.

$$NRMSE = \frac{1}{A}\sqrt{\frac{1}{np}\sum_{k=1}^{np}\left(\hat{f}_{u,k} - f_{u,k}\right)^2} \tag{24}$$

where A is the amplitude of force; np is the number of sampling points, $\hat{f}_{u,k}$ and $f_{u,k}$ denote the identified input and actual input at the k-th time step, respectively. In this

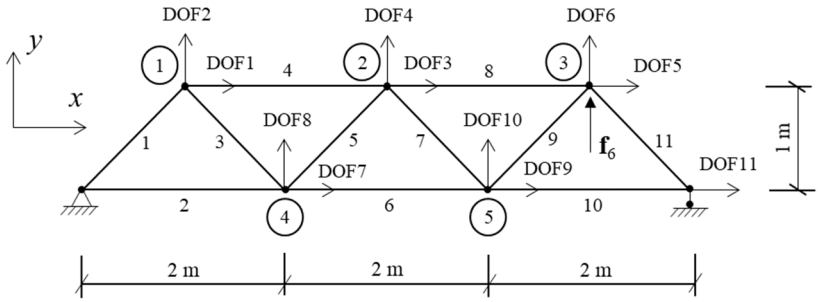

Fig. 4 The planar truss structure

example, the values of NRMSE of the unknown inputs applied on the 2nd and 8th floor are 1.02% and 1.21%, receptively, indicating that the identified forces are close to the actual ones.

3.2 Planar truss structure

A planar truss structure as shown in Fig. 4 is considered. In this example, the case of only implicit unknown input being involved is discussed. The truss structure consists of 11 members with the same cross-sectional area of 2×10^{-3} m^2. The Young's module is selected as 2×10^8 Pa, and mass density is 7850 kg/m^3. The consistent mass distribution is employed for the construction of the mass matrix. The Rayleigh damping assumption is used, and the proportional coefficients are assumed as $\alpha = 0.949$ and $\beta = 8 \times 10^{-4}$. The first two damping ratios are 3%, and the first three natural frequencies are 3.71 Hz, 7.83 Hz, 11.63 Hz, respectively.

A random force is applied at the DOF6 as shown in Fig. 4, and the corresponding structural responses are calculated

Table 2 The identified structural parameters of truss structure

Parameters (kN/m)	Actual	Identified	Error (%)	Parameters (kN/m)	Actual	Identified	Error (%)
k_1	282.84	283.12	0.10	k_8	200.00	199.28	-0.36
k_2	200.00	198.27	-0.86	k_9	282.84	282.74	-0.04
k_3	282.84	282.42	-0.15	k_{10}	200.00	199.80	-0.10
k_4	200.00	200.28	0.14	k_{11}	282.84	282.64	-0.07
k_5	282.84	282.596	-0.09	α	0.949	0.9224	-2.80
k_6	200.00	201.45	0.72	β	0.0008	0.0008	-
k_7	282.84	283.08	0.08				

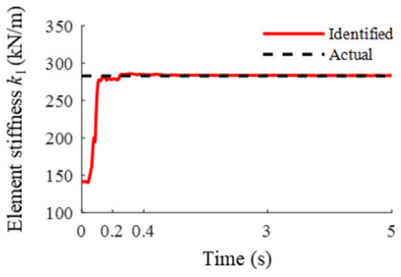

(a) k_1

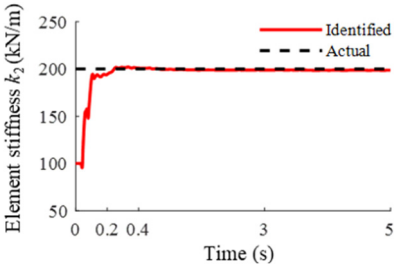

(b) k_2

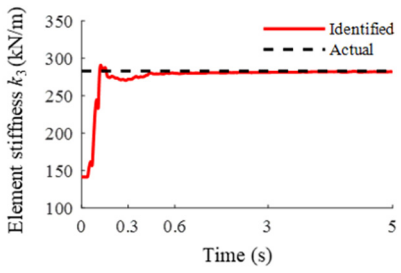

(c) k_3

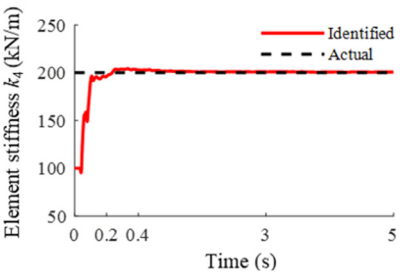

(d) k_4

Fig. 5 The identified stiffness of truss structure

by state-space method with the time interval of 0.001 s. The acceleration responses of the 1st, 2nd, 3rd, 4th, 8th, 9th, 10th and 11th DOF and the displacement responses of the 5th and 7th DOF are used for the identification. The noise level is also assumed to be 5%. The unknown parameters include the stiffness of the 11 elements and two Rayleigh damping coefficients. By using the proposed approach, the structural parameters are identified and listed in Table 2. A good agreement between the identified values and the actual ones can be observed. Fig. 5 gives the convergence procedure of some identified parameters. Due to space limitation, only the identified stiffness of the 1st element to 4th element is plotted as examples. It can be seen that the identified values can promptly and stably converge to the actual ones. Similar results can be observed for the remaining parameters.

The unknown external excitation can be also identified by the proposed approach. Notably, since the acceleration at the 6th DOF is not measured, the external force at node 3 (i.e., $\mathbf{f}_6$ as shown in Fig. 4) can be viewed as an implicit unknown input. It can be also found that there is no explicit unknown input in this example. Thus, the implicit unknown input can be determined by using Eq. (23) with the consideration of $\hat{\boldsymbol{f}}^*_{u,k+1}$ and $\hat{\boldsymbol{f}}^*_{u,k}$ being zero. The identified input is shown in Figs. 6(a)-(b) as solid line, whereas the real one is plotted as dashed line. The time segment from 4 s to 5 s is also given in Fig. 6 for clarity of comparison. The value of NRMSE defined in Eq. (23) is 0.83% in this example. It can be seen the identified input is quite close to the real one.

3.3 Shear building with a nonlinear hysteretic model

In this section, the identification of structural parameters in the nonlinear system is discussed. The same shear building introduced in section 3.1 is employed herein. The structural parameters are set as m_i = 180 kg, k_i = 550 kN/m (i = 1, …, 8), α = 0.457 and β = 1.5 × 10^{-3}. A hysteretic Dahl model is assumed to be installed on the 5th floor to mimic local nonlinearity. The nonlinear restoring force provided by Dahl model in this case can be expressed as

$$\boldsymbol{F}_{Dahl} = k_D \Delta \boldsymbol{x}_5 + c_D \Delta \dot{\boldsymbol{x}}_5 + f_D \boldsymbol{z}_D + f_0 \tag{25}$$

where k_D and c_D are stiffness and damping coefficients of the Dahl model, respectively; f_D and f_0 are force coefficients; $\Delta \mathbf{x}_5$ and $\Delta \dot{\boldsymbol{x}}_5$ are the relative displacement and relative velocity of the 5th floor, respectively; $\mathbf{z}_D$ is a dimensionless quantity used to describe Coulomb friction as

$$\dot{\boldsymbol{z}}_D = \sigma_D \cdot \Delta \dot{\boldsymbol{x}}_5 \cdot [1 - \boldsymbol{z}_D \cdot \mathrm{sign}(\Delta \dot{\boldsymbol{x}}_5)] \tag{26}$$

where σ_D is the parameter used to control the shape of hysteresis loop; sign(·) denotes signum function. In this study, the parameters of Dahl model are set as k_D = 50 N/m, c_D = 400 N·s/m, f_D = 300 N, f_0 = 0N, and σ_D = 1000 s/m.

An external excitation is applied on the 3rd floor of the building, and the corresponding nonlinear responses are calculated by Runge-Kutta method with the time interval of 0.001 s. The acceleration responses of the 1st, 2nd, 4th, 5th, 6th and 8th floor as well as displacement response of the 2nd are used for the identification. All the measurements are assumed to be contaminated by 5% noise. The extended

(a) The entire time series (b) Time segment from 4 s to 5 s

Fig. 6 The comparison of the identified force applied to truss structure

Table 3 The identified parameters of nonlinear system

Parameters (kN/m)	Actual	Identified	Error (%)	Parameters (kN/m)	Actual	Identified	Error (%)
k_1 (kN/m)	550	535.79	-2.58	k_8 (kN/m)	550	534.42	-2.83
k_2 (kN/m)	550	552.82	0.51	k_D (N/m)	50	49.54	-0.91
k_3 (kN/m)	550	541.83	-1.48	c_D (N·s/m)	400	396.47	-0.88
k_4 (kN/m)	550	544.50	-1.00	f_D (N)	300	294.26	-1.91
k_5 (kN/m)	550	531.00	-3.45	σ_D (s/m)	1000	989.80	-1.02
k_6 (kN/m)	550	541.24	-1.59	α	0.4577	0.4634	1.23
k_7 (kN/m)	550	557.24	1.31	β	0.0015	0.0015	-

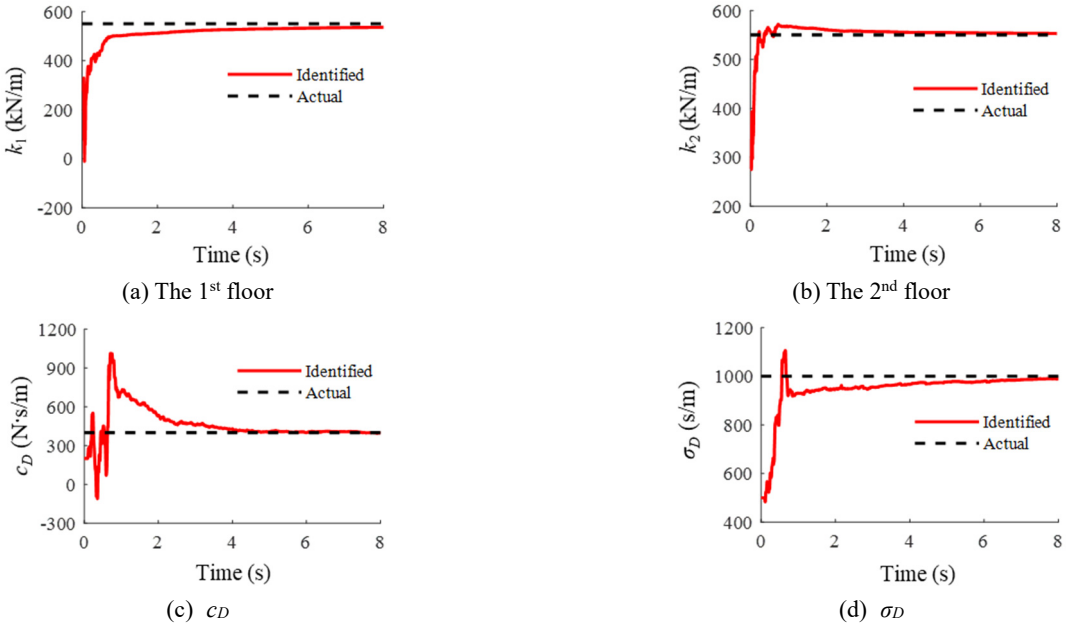

(a) The 1st floor (b) The 2nd floor

(c) c_D (d) σ_D

Fig. 7 The identified parameters of nonlinear system

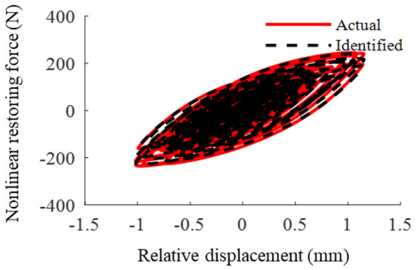

Fig. 8 The nonlinear restoring force provided by Dahl model

state vector is defined a $\boldsymbol{Z} = [x_1,\ldots,x_8,\ \dot{x}_1,\ldots,\dot{x}_8,\ k_1,\ldots,k_8,\ k_D,\ c_D,\ f_D,\ \sigma_D,\ \alpha,\ \beta]^T$. The initial values of the unknown parameters are set to be 50% of the corresponding actual ones.

Based on the aforementioned information, the unknown parameters can be identified by the proposed approach as shown in Table 3. It can be seen that as compared with the linear case, the identification errors in the nonlinear system are relatively large. Even so, the results are still acceptable with the maximum error only being 3.45%. Fig. 7 gives the time histories of some parameters to show their convergence processes. It is clear that the identified parameters can converge to their actual ones after few seconds. Similar results can be found for the remaining parameters. Based on the identified parameters of Dahl model and the estimated structural states, the nonlinear restoring force provided by Dahl model can be also obtained. The hysteretic performance of Dahl model is shown in Fig. 8 for comparison. Obviously, the estimated nonlinear restoring force matches with the theoretical one very well.

The unknown excitation can be estimated by the proposed approach as well. Notably, the force applied to the 3rd flood should be treated as implicit unknown input due to the acceleration of this floor being unmeasured. Also, there is no explicit unknown input involved in this example. The comparison of the identified excitation with the real one is depicted in Fig. 9. The time segment from 7 s to 8 s is also given for clarity of comparison. The value of NRMSE in this case is 2.24%. Although the NRMSE value is relatively larger than that of linear case, it can be concluded that the proposed approach is still capable of identifying unknown loads even structural nonlinearity involved.

(a) The entire time series (b) Time segment from 7 s to 8 s

Fig. 9 The comparison of the identified force in nonlinear system

4. Conclusions

According to whether the external forces are presented in observation equation or not, these unknown inputs can be divided into two parts in this study, namely explicit unknown inputs and implicit unknown inputs. Many available EKF-UI methods are basically performed on the premise that collocated acceleration measurements at the locations of unknown inputs are measured. Thus, these methods are not applicable if the implicit unknown inputs are involved. In this paper, an improved extended Kalman filter with unknown input (IEKF-UI) is proposed for identifying the structural parameters and unknown inputs at the same time. An improved observation equation is obtained with the aid of projection matrix and data fusion technique. By using FOHD method for discretizing continuous function and Taylor series for linearization procedure, the implicit inputs can be directly identified without the requirement of collocated acceleration response measurements. As compared with many existing EKF-UI methods, a merit of the proposed approach is that the restriction on the sensor locations is removed. Numerical examples show that the proposed approach is capable of simultaneously identifying the parameters of linear/nonlinear structures as well as the unknown inputs applied to them. It should be noted that in order to obtain the improved observation equation, the mass matrix should be known in the proposed approach. Further research can be conducted for the parameter and force identification without the prior knowledge of mass distribution. Moreover, dynamic tests can be carried out to verify the effectiveness of the approach for real structural model.

Acknowledgments

The financial support from the National Key Research and Development Program of China (grant number 2019YFC1511101) is greatly appreciated. The support from National Natural Science Foundation of China (No. 52278305), Natural Science Foundation of Hunan Province (No. 2021JJ30110) and Innovation Platform Open Fund project of Hunan Province (No. 19K018) is also greatly appreciated.

References

Chatzis, M.N., Chatzi, E.N. and Triantafyllou, S.P. (2017), "A discontinuous extended Kalman filter for non-smooth dynamic problems", *Mech. Syst. Signal Process*, **92**, 13-29. https://doi.org/10.1016/j.ymssp.2017.01.021

Das, S. and Saha, P. (2018), "Structural health monitoring techniques implemented on IASC–ASCE benchmark problem: a review", *J. Civil Struct. Health Monit.*, **8**(4), 689-718. https://doi.org/10.1007/s13349-018-0292-5

Ding, Y., Law, S.S., Wu, B., Xu, G.S., Lin, Q., Jiang, H.B. and Miao, Q.S. (2013), "Average acceleration discrete algorithm for force identification in state space", *Eng. Struct.*, **56**, 1880-1892. https://doi.org/10.1016/j.engstruct.2013.08.004

Ginsberg, D., Fritzen, C.P. and Loffeld, O. (2018), "Sparsity-constrained extended Kalman filter concept for damage localization and identification in mechanical structures", S*mart Struct. Syst.*, *Int. J.*, **21**(6), 741-749. https://doi.org/10.12989/sss.2018.21.6.741

Hannan, M.A., Hassan, K. and Jern, K.P. (2018), "Review on sensors and systems in structural health monitoring: current issues and challenges", *Smart Struct. Syst.*, *Int. J.*, **22**(5), 509-525. https://doi.org/10.12989/sss.2018.22.5.509

He, J., Zhang, X.X and Xu, B. (2019a), "Identification of structural parameters and unknown inputs based on revised observation equation: approach and validation", *Int. J. Struct. Stab. Dyn.*, **19**(12), 1950156. https://doi.org/10.1142/S0219455419501566

He, J., Zhang, X.X. and Dai, N.X. (2019b), "An improved Kalman filter for joint estimation of structural states and unknown loadings", *Smart Struct. Syst.*, *Int. J.*, **24**(2), 209-221. https://doi.org/10.12989/sss.2019.24.2.209

He, J., Zhang, X.X., Feng, Z.Q., Chen, Z.Q. and Cao, Z. (2020), "A two-stage Kalman filter for the identification of structural parameters with unknown loads", *Smart Struct. Syst.*, *Int. J.*, **26**(6), 693-701. https://doi.org/10.12989/sss.2020.26.6.693

He, J., Qi, M.C, Hua, X.G, Chen, Z.Q, Yang, O. and Cao, Z. (2021), "Substructural identification with weighted global iteration considering unknown interfacial forces and external excitation", *Measurement*, **180**, 109537. https://doi.org/10.1016/j.measurement.2021.109537

Hoshiya, M. and Saito, E. (1984), "Structural identification by extended Kalman filter", *J. Eng. Mech.*, **110**(12), 1757-1770. https://doi.org/10.1061/(ASCE)0733-9399(1984)110:12(1757)

Lai, Z., Lei, Y., Zhu, S.Y., Xu, Y.L., Zhang, X.H. and Krishnaswamy, S. (2016), "Moving-window extended Kalman filter for structural damage detection with unknown process and measurement noises", *Measurement*, **88**, 428-440. https://doi.org/10.1016/j.measurement.2016.04.016

Lei, Y., Jiang, Y. and Xu, Z. (2012), "Structural damage detection with limited input and output measurement signals", *Mech. Syst. Signal Proc.*, **28**, 229-243. https://doi.org/10.1016/j.ymssp.2011.07.026

Lei, Y., Lai, Z., Zhu, S. and Zhang, X.H. (2014), "Experimental study on impact-induced damage detection using an improved extended Kalman filter", *Int. J. Struct. Stab. Dyn.*, **14**(5), 1440007. https://doi.org/10.1142/S0219455414400070

Lei, Y., Xia, D.D., Chen, F. and Deng, Y.M. (2018), "Synthesis of cross-correlation functions of partial responses and the extended Kalman filter approach for structural damage detection under ambient excitations", *Int. J. Struct. Stab. Dyn.*, **18**(8), 1840003. https://doi.org/10.1142/S0219455418400035

Lei, Y., Lu, J., Huang, J. and Chen, S. (2020), "A general synthesis of identification and vibration control of building structures under unknown excitations", *Mech. Syst. Signal Proc.*, **143**, 106803. https://doi.org/10.1016/j.ymssp.2020.106803

Lei, Y., Yang, X., Huang, J., Zhang, F. and Liu, L. (2021), "Identification of model-free hysteretic forces of magnetorheological dampers embedded in buildings under unknown excitations using incomplete structural responses", *Struct. Control Health Monit.*, **28**(5), e2715. https://doi.org/10.1002/stc.2715

Li, D. and Wang, Y. (2020), "Parameter identification of a differentiable Bouc-Wen model using constrained extended Kalman filter", *Struct. Health Monit.*, **20**(1), 360-378. https://doi.org/10.1177/1475921720929434

Liu, L., Lei, Y. and He, M. (2016), "A two-stage parametric identification of strong nonlinear structural systems with incomplete response measurements", *Int. J. Struct. Stab. Dyn.*, **16**(4), 1640022. https://doi.org/10.1142/S0219455416400228

Liu, L., Hua, W. and Lei, Y. (2018), "Real-time simultaneous identification of structural systems and unknown inputs without collocated acceleration measurements based on MEKF-UI",

Measurement, **122**, 545-553. https://doi.org/10.1016/j.measurement.2017.07.001

Mu, H.Q. and Yuen, K.V. (2015), "Novel outlier-resistant extended Kalman filter for robust online structural identification", *J. Eng. Mech.*, **141**(1), 04014100. https://doi.org/10.1061/(ASCE)EM.1943-7889.0000810

Naranjo-Perez, J., Jimenez-Alonso, J.F. and Saez, A. (2020), "Parameter identification of the dynamic Winkler soil-structure interaction model using a hybrid unscented Kalman filter-multi-objective harmony search algorithm", *Adv. Struct. Eng.*, **23**(12), 2653-2668. https://doi.org/10.1177/1369433220919074

Pan, S., Xiao, D., Xing, S., Law, S.S., Du, P. and Li, Y. (2016), "A general extended Kalman filter for simultaneous estimation of system and unknown inputs", *Eng. Struct.*, **109**, 85-98. https://doi.org/10.1016/j.engstruct.2015.11.014

Saleem, M.M. and Jo, H. (2019), "Impact force localization for civil infrastructure using augmented Kalman Filter optimization", *Smart Struct. Syst., Int. J.*, **23**(2), 123-139. https://doi.org/10.12989/sss.2019.23.2.123

Saleem, M.M. and Jo, H. (2021), "Multi-objective sensor placement optimization for structural response estimation under spatially varying dynamic loading of bridges", *Adv. Struct. Eng.*, **24**(10), 2255-2266. https://doi.org/10.1177/1369433221993574

Xiao, X., Xu, X. and Shen, W. (2021), "Simultaneous identification of the frequencies and track irregularities of high-speed railway bridges from vehicle vibration data", *Mech. Syst. Signal Proc.*, **152**, 107412. https://doi.org/10.1016/j.ymssp.2020.107412

Xu, B. and He, J. (2015), "Substructural parameters and dynamic loading identification with limited observations", *Smart Struct. Syst., Int. J.*, **15**(1), 169-189. https://doi.org/10.12989/sss.2015.15.1.169

Xu, Y.L. and He, J. (2017), *Smart Civil Structures*, CRC Press, Boca Raton, FL, USA.

Xu, Y.L., Zhang, X.H., Zhu, S. and Zhan, S. (2016), "Multi-type sensor placement and response reconstruction for structural health monitoring of long-span suspension bridges", *Sci. Bull.*, **61**(4), 313-329. https://doi.org/10.1007/s11434-016-1000-7

Xu, B., Li, J., Dyke, S.J., Deng, B.C. and He, J. (2020), "Nonparametric identification for hysteretic behavior modeled with a power series polynomial using EKF-WGI approach under limited acceleration and unknown mass", *Int. J. Non-Linear Mech.*, **119**, 103324. https://doi.org/10.1016/j.ijnonlinmec.2019.103324

Yang, J.N., Pan, S. and Huang, H. (2007), "An adaptive extended Kalman filter for structural damage identifications II: Unknown inputs", *Struct. Control Health Monit.*, **14**(3), 497-521. https://doi.org/10.1002/stc.171

Yang, Y., Nagayama, T. and Xue, K. (2020), "Structure system estimation under seismic excitation with an adaptive extended Kalman filter", *J. Sound Vib.*, **489**, 115690. https://doi.org/10.1016/j.jsv.2020.115690

Yun, C.B. and Shinozuka, M. (1980), "Identification of nonlinear structural dynamic systems", *J. Struct. Mech.*, **8**(2), 187-203. https://doi.org/10.1080/03601218008907359

Zhang, C., Huang, J.Z., Song, G.Q. and Chen, L. (2017), "Structural damage identification by extended Kalman filter with l1-norm regularization scheme", *Struct. Control Health Monit.*, **24**(11), 1-17. https://doi.org/10.1002/stc.1999

Zhang, X.H., Zhu, Z., Yuan, G.K. and Zhu, S.Y. (2021), "Adaptive mode selection integrating Kalman filter for dynamic response reconstruction", *J. Sound Vib.*, **515**, 116497. https://doi.org/10.1016/j.jsv.2021.116497